Journal of Applied Electrochemistry (2006) 36:1311–1315
DOI 10.1007/s10800-005-9101-z

The inhibition of copper–nickel alloy corrosion under controlled hydrodynamic condition in seawater

S. MARTINEZ and M. METIKOŠ-HUKOVIĆ*
Department of Electrochemistry, Faculty of Chemical Engineering and Technology, University of Zagreb, PO Box 177, Zagreb, 10000, Croatia
*(*author for correspondence, tel.: + 385-1-4597-140, fax: + 385-1-4597-139, e-mail: mmetik@marie.fkit.hr)*

Received 20 April 2005; accepted in revised form 21 November 2005

Key words: chelate complex, copper alloys, corrosion, hydrodynamic conditions, inhibitor, jet impingement attack, sodium-diethyl-dithiocarbamate

Abstract

A comparative study of the corrosion resistance of a bare Cu–10 Ni alloy and a Cu–10 Ni alloy protected by sodium-diethyl-dithiocarbamate ($NaEt_2dtc$) has been undertaken. The experimental conditions varied from quiescent natural seawater to seawater subjected to jet impingement of different fluid velocities. The mechanism of inhibitor action has been suggested that includes the formation of a surface chelate compound between the dissolving metal ion and the $(Et_2dtc)^-$ ligand, as well as formation of a 3-D ternary surface complex. The surface layer that incorporates both the inhibitor and the cuprous oxide, represented by the structure:

Cu–Ni/Cu_2O/Cu(II) organic complex/seawater

has shown an excellent protective performance with efficiency >90% under stagnant and fluid impingement conditions.

1. Introduction

Cu–Ni alloys, also known as cupronickels, have been used for over 60 years in saline environments, e.g. as construction materials for seawater piping, heat exchangers and condensers in ships, desalination plants, power plants, as protective layers on oil platforms and ship hulls etc. This extensive use has triggered numerous investigations of these alloys with the aim of improving their performance under various conditions [1–5]. Many applications of cupronickels involve flow of the corrosive fluid and these alloys are known to suffer accelerated corrosion when exposed to flowing electrolyte [6]. It is therefore of a particular interest to perform laboratory measurements under a hydrodynamic regime that effectively simulates service conditions [7, 8]. Generally, action of a corrosion inhibitor can be related to its molecular spatial structure and molecular electronic structure as well as to its hydrophobicity, solubility, dispersibility and ability to form metal chelates [9, 10].

Some complexing agents have proved to be beneficial to the corrosion stability of cupronickels [11–13]. In particular, sodium-diethyl-dithiocarbamate ($NaEt_2dtc$), known to be highly versatile chelating agent, has been investigated on pure Cu [12] and Cu–10 Ni alloy [13] and has shown excellent performance in quiescent saline solutions.

The objective of this work was to perform a comparative study of the corrosion resistance of a bare Cu–10 Ni alloy and one protected by sodium-diethyl-dithiocarbamate, in quiescent natural seawater and under the influence of seawater jet impingement of various fluid velocities. The purpose was to identify sodium-diethyl-dithiocarbamate as a candidate inhibitor of Cu–10 Ni alloy in flowing saline systems with the perspective of further long-term investigations that would more realistically simulate conditions in an industrial environment. In our previous publications the passivity and susceptibility of Cu–Ni alloy containing (10, 20, 30 and 40% Ni) as well as of pure metal components to localized, pitting, and corrosion have been extensively studied [14–16]. Inhibition of the anodic dissolution of Cu and Cu–10 Ni alloy in a 1 M sodium acetate solution pH 5.8 in the presence of different concentrations of benzotriazole was studied using spectroelectrochemical methods. The excellent inhibition efficiency of benzotriazole was due to the formation of a surface film of a dielectric nature [17].

2. Experimental details

Cu–10 Ni alloy was prepared from pure Cu and Ni constituents (99.99%). The metals were homogenized for 4 h at 350 °C, rolled and then annealed for 1 h at 650 °C. Samples were machined in the form of cylinders, 15 mm in diameter and 2 mm thick. Analytical grade ($NaEt_2dtc$) was obtained from Sigma. Electrolyte was filtered natural seawater pH 7.9. For electrochemical measurements in natural seawater the pretreatment of each specimen consisted of gradual polishing, starting with fine grained emery papers and alumina powder down to 0.05 μm grain size. Polishing was followed by rinsing, degreasing in isopropyl alcohol vapor and in ethanol in the ultrasonic bath. The specimens were then dried in a stream of nitrogen, before immersion in ($NaEt_2dtc$) solution. During the prolonged contact with an electrolyte solution at the open circuit potential and at $c(NaEt_2dtc) = 26.6\times10^{-4}$ mol dm^{-3} a protective film was formed on the Cu–10 Ni specimen surface [13]. After 24 h immersion at 25 °C the electrodes were air dried prior to exposure to an environment.

Electrochemical corrosion measurements were carried out at 25 °C using a modified PAR corrosion cell (Figure 1) where a combination of circulating pump and jet nozzle (diam. = 1 mm) was set up to simulate jet impingement attack [8]. The separation distance between the tip of the nozzle and the working electrode was fixed at 3 mm. Polarization measurements were performed on all specimens after 30 min of exposure to the environment. A saturated calomel electrode served as a reference electrode and two graphite rods served as counter electrodes. The electrochemical behavior was studied by combined potentiodynamic and quasi potentiostatic methods. In the first case the potential was scanned at a rate of 1 mV s^{-1} from the corrosion potential, E_{corr} into the cathodic and anodic potential region ($E = \pm250$ mV E_{corr}). Small amplitude voltammetry (linear polarization) was obtained by imposing a small amplitude ($E = \pm15$ mV E_{corr}) potential excitation at the corrosion potential. The voltage sweep rate was 0.3 mV s^{-1}. The experiments were conducted repeatedly under the same conditions and reproducibility of results was very good.

3. Results

Figures 2 and 3 show polarization curves as Tafel plots of non-protected and protected alloy samples, respectively, in stagnant natural seawater and under the influence of the seawater jet impingement. Anodic and cathodic current densities are significantly higher in the fluid flow system with respect to those in the stagnant system for non-protected Cu–Ni electrodes. Typical small amplitude voltammograms (linear polarization method) recorded in a narrow potential range in the vicinity of the corrosion potential are shown in Figures 4 and 5. At a scan rate of 0.3 mV s^{-1} straight lines with constant slopes were obtained.

Corrosion kinetic parameters and the corrosion rate for Cu–10 Ni electrodes were deduced from polarization curves using Tafel and polarization resistance methods. It was shown by Wagner and Trand and by Mansfeld and Oldham [18] that for a polarization curve of the form

$$j = j_{corr}\left[e^{\frac{2.3(E-E_{corr})}{b_a}} - e^{\frac{2.3(E-E_{corr})}{b_c}}\right] \quad (1)$$

the corrosion current, j_{corr} is proportional to the slope of the polarization curve at the corrosion potential, E_{corr}

$$j_{corr} = \frac{1}{2.3}\frac{b_a b_c}{b_a + b_c}\left(\frac{dj}{dE}\right)_{E_{corr}} = \frac{B}{R_p A} \quad (2)$$

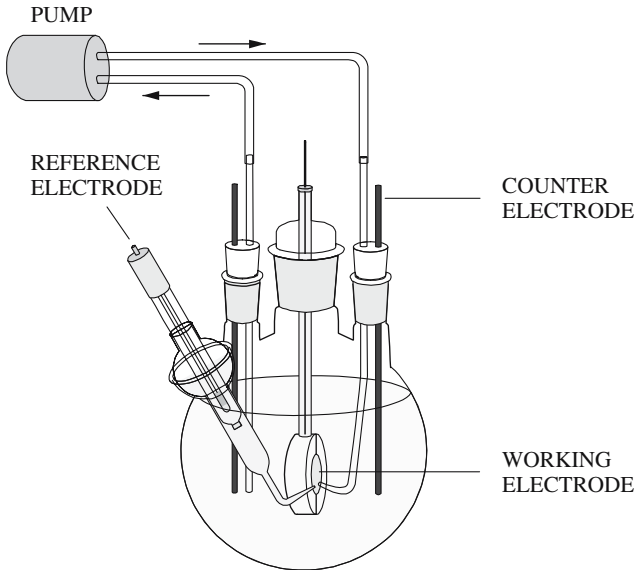

Fig. 1. The electrochemical reactor utilized in the experimental method.

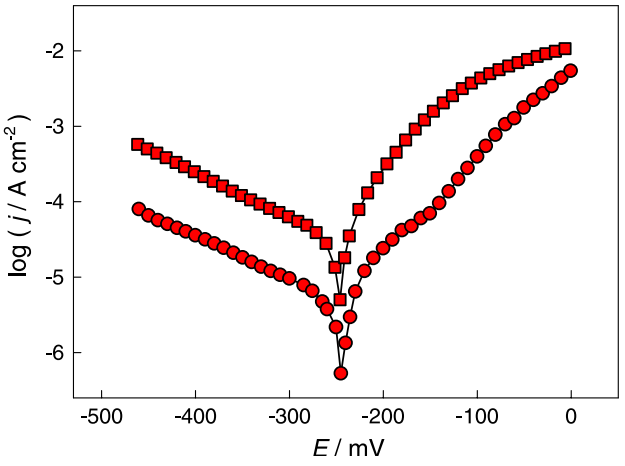

Fig. 2. Polarization curves of the Cu–10 Ni non-protected electrode in stagnant natural seawater (●) and under the influence of the seawater jet impingement with the fluid velocity 8.3 m s^{-1} (■). Scan rate was 1 mV s^{-1}.

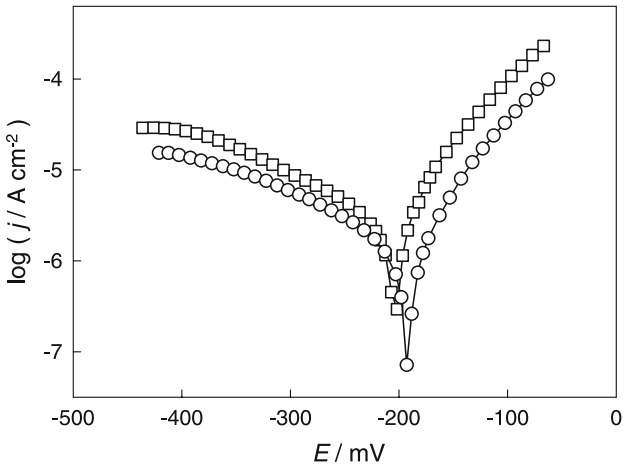

Fig. 3. Polarization curves of the Cu–10 Ni protected electrode in stagnant natural seawater (●) and under the influence of the seawater jet impingement with the fluid velocity 8.3 m s^{-1} (■). Scan rate was 1 mV s^{-1}.

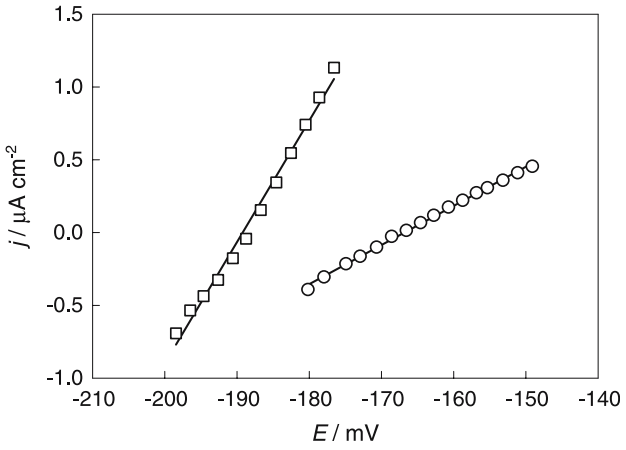

Fig. 5. Small amplitude voltammogram-lined polarisation plot obtained in polarization curves of the Cu–10 Ni non-protected electrode in stagnant natural seawater (○) and under the influence of the seawater jet impingement with the fluid velocity 8.3 m s^{-1} (□). Scan rate was 0.3 mV s^{-1}.

where $E-E_{corr}=\eta$ is the overpotential, R_p is the polarization resistance and A is the geometric electrode area.

Corrosion potential, corrosion rate, anodic and cathodic Tafel slopes (b_a and b_c) obtained for Cu–Ni electrodes in natural seawater as a function of fluid velocities (the flow velocities) are shown in Table 1. The corrosion parameters for protected Cu–Ni electrodes are listed in Table 2. The data obtained in stagnant natural seawater are included in Tables 1 and 2 for comparison with the measured corrosion parameters under hydrodinamic conditions (simulated impingement conditions).

The corrosion current density, j_{corr} (Tafel method) and the reciprocal value of the polarization resistance R_p^{-1} were used as a measure of the corrosion rate. On the unprotected electrode surface, j_{corr} is by an order of magnitude higher in the system with fluid flow than in the stagnant system (Table 1). The corrosion rate on the protected Cu–Ni electrode surface is two orders of magnitude lower than the corrosion rate of the unprotected electrode in the range of fluid velocity studied (Table 2).

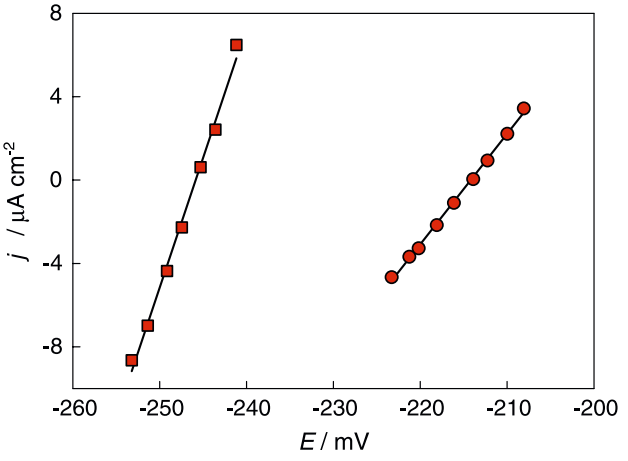

Fig. 4. Small amplitude voltammogram (linear polarization plot) of the Cu–10 Ni non-protected electrode in stagnant natural seawater (○) and under the influence of the seawater jet impingement with the fluid velocity to 8.3 m s^{-1} (□). Scan rate was 0.3 mV s^{-1}.

The high values of the cathodic Tafel slope, b_c for both electrode surfaces ($b_c \approx 170$ mV and $b_c \approx 200$ mV) is believed to be caused by the presence of a corrosion product layer at the surface. Its protection against corrosion attack under simulated impingement conditions is markedly improved after Cu–Ni treatment in a (Na_2Et_2dtc) solution.

The presence of the film on the Cu–10 Ni electrode surface and the fluid velocity does not significantly influence the anodic Tafel slope, b_a (Tables 1 and 2). The values of b_a are of about 60 mV dec^{-1} and indicating a two-electron transfer anodic reaction.

4. Discussion

On the non-protected electrode surface, the corrosion rate is two orders of magnitude higher than on the protected electrode surface in the system with fluid flow. A comparative plot of polarization curves obtained on the non-protected and protected Cu–10 Ni electrodes for the fluid velocity 8.3 m s^{-1} is shown in Figure 6. The inhibitor efficiency calculated from corrosion currents and polarization potentials is shown in Table 3. The protected film influences the corrosion process at the electrode/electrolyte interface. Therefore, the steady-state corrosion potential, E_{corr} is shifted about 30 mV to more positive potentials in comparison with the unprotected electrode as shown in Figure 6. Copper–Nickel alloys containing up to 40% of Ni have good corrosion resistance mainly due to the formation of the protective barrier layer of Cu_2O which is a *p*-type semiconductor [16]. In chloride solutions, it has been reported that above this oxide layer, there is an atacamite $Cu_2(OH)_3Cl$ film [1–3, 14, 15]. Generally, the presence of chelating ligands in electrolyte solution leads to modification of the outer part of the surface

Table 1. Corrosion parameters of the Cu–10 Ni non-protected electrode deduced from polarization measurements in natural seawater for various fluid velocities at the tip of the nozzle

Fluid velocity/m s^{-1}	Corrosion potential/mV	Corrosion current/A cm^{-2}	Anodic Tafel slope/mV dec^{-1}	Cathodic Tafel slope/mV dec^{-1}	Polarization resistance/k Ω cm^2
0	−248.86	4.69×10^{-6}	73.49	−170.43	1.83
2.7	−248.02	2.20×10^{-5}	56.08	−195.13	1.31
6.4	−248.21	2.48×10^{-5}	56.20	−175.20	0.91
8.3	−249.81	3.13×10^{-5}	55.55	−172.67	0.68

Table 2. Corrosion parameters of the Cu–10 Ni protected electrode deduced from polarization measurements in natural seawater for various fluid velocities at the tip of the nozzle

Fluid velocity/s^{-1}	Corrosion potential/mV	Corrosion current/A cm^{-2}	Anodic Tafel slope/mV dec^{-1}	Cathodic Tafel slope/mV dec^{-1}	Polarization resistance/k Ω cm^2
0	−186.57	9.39×10^{-6}	61.18	−131.60	37.75
2.7	−195.23	2.23×10^{-7}	65.22	−193.31	22.77
6.4	−195.71	2.29×10^{-7}	66.70	−199.71	13.10
8.3	−203.73	2.61×10^{-7}	65.92	−228.84	11.59

layer via a complexation process [19]. The high inhibition efficiency of the corrosion attack observed in both stagnant and flow systems suggest that an insoluble film is formed at the electrode surface during the prolonged exposure of the Cu–10 Ni surface to a ($NaEt_2dtc$) solution. The finding that the $(Et_2dtc)^-$ ligand is a very efficient inhibitor in both stagnant and flows systems may be attributed to the strong complexing power for Cu^{2+} ions at the reactive oxide surface and formation of an insoluble film at the electrode-solution interface.

The $DETTC^-$ ligand is known to form chelates with virtually all transition elements [20]. Investigation of the molecular properties of dialkyl-dithiocarbamates and their chelates with metal ions has been, due to their growing applications in analytical chemistry, industry, biology and medicine, an important goal of many researchers [20–24].

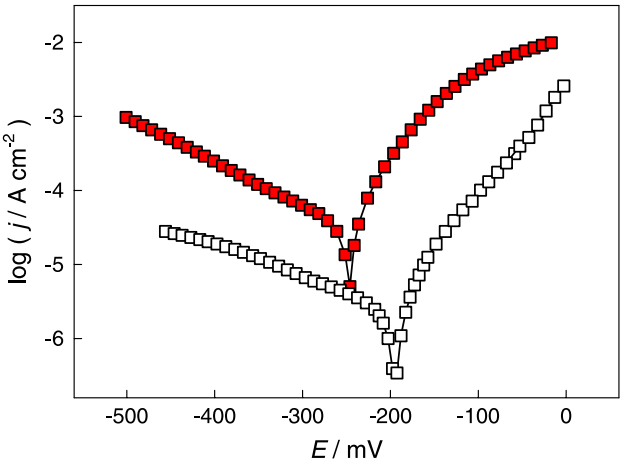

Fig. 6. Comparative plot of polarization curves obtained on the non-protected Cu–10 Ni electrode (■) and on the protected Cu–10 Ni electrode (□) under the influence of the seawater jet impingement with the fluid velocity 8.3 m s^{-1}. Scan rate was 1 mV s^{-1}.

In some instances, the formation of metal–ligand complexes can promote metal dissolution, keeping metal ions in the dissolved phase and rendering them highly mobile [25, 26]. However, adsorption of the complexed metal, forming a ternary complex may occur under specific conditions. The resulting ternary complex can be exceedingly stable and possess properties very different from those of the individual component species. These differences can have significant implications in a number of natural and engineering processes [25–30]. In particular, surface chelates have been known to play a significant role in corrosion inhibition [12, 31–34]. For example, tannin stimulates iron dissolution in a neutral borate buffer solution due to its ability to form chelate bonds with Fe(II) ions by autocatalytic process. However, the TanFe(II) complex easily converts by dissolved oxygen into TanFe(III) complex, which contributes to iron passivation by forming an insoluble chelating complex [35].

Upon exposure of the Cu–10 Ni surface to a ($NaEt_2dtc$) solution, a surface insoluble film starts to develop within minutes, causing a specific reddish-brown surface coloration that is distinctively different form those formed in inhibitor free solution. AES results confirm the concomitant existence of Cu_2O and the inhibitor in the surface film [36]. For the proposed inhibition mechanism, chelate ring formation is necessary, which is corroborated by the above observation as

Table 3. Inhibitor efficiency in stagnant natural seawater and for various fluid velocities at the tip of the nozzle

Fluid velocity/m s^{-1}	Inhibitor efficiency from corrosion currents/%	Inhibitor efficiency from polarization resistance/%
0	95.15	79.99
2.7	94.21	89.87
6.4	93.22	90.78
8.3	95.50	91.69

well as by the results of Singh et al. [12, 34] showing that dithiocarbamates and their Cu(II) complexes exert almost identical inhibitor efficiency. Recently, Ochoa et al. [32] have found that chelate formation at the oxide-hydroxide layer improves its protective properties under electrolyte flow conditions.

The chemical structure of diethyl-dithiocarbamate absorbed onto cuprous oxide may involve 1:1 and 1:2 metal:ligand ratios i.e. mono- and bis-bidentate complexes (CuRdtc) and lipophilic neutral $Cu(R_2dtc)_2$) and possibly 2:1 metal:ligand ratios (binuclear complex) [20–24]. Five-membered ring chelates are favored in coordination for steric and entropic reasons. The ''bite'' (S–S) distance in the carbamate ligand of 2.98 Å may be compatible with surface Cu–Cu distances in Cu_2O of 3.01 Å [37], suggesting that diethyl-dithiocarbamate may also form a binuclear precursor surface.

5. Conclusions

It is well-known that the corrosion resistance of Cu–Ni alloys in aqueous solutions, without the presence of complexing additives or corrosion activators, such as Cl^- ions, depends mainly on the formation of a protective Cu_2O barrier layer. In the presence of Cl^- ions an outer more soluble layer of $Cu(OH)_3Cl$ is established on the top of Cu_2O inner layer.

Our investigations clearly show that the leaching of Cu^{2+} at the solid/liquid interface can be inhibited with the addition of the $(Et_2dtc)^-$ chelating species, which form a stable, insoluble complex at the electrode surface. The protective surface layer formed upon exposure of the Cu–10 Ni alloy to the Na_2Et_2dtc solution incorporates both Cu_2O and organic complex: Cu–Ni/Cu_2O/Cu(II) organic complex/seawater.

A systematic study carried out in this work to investigate the effect of hydrodynamic conditions on the corrosion resistance of the Cu–10 Ni alloy in natural seawater has shown an excellent protective performance of the 3-D surface layer under stagnant and fluid impingement conditions. The investigated compound is a good candidate corrosion inhibitor for Cu–Ni marine alloys under various hydrodynamic conditions with excellent inhibiting efficiency (>90%).

References

1. R.G. Blundy and M.J. Pryor, *Corros. Sci.* **12** (1972) 65.
2. H. Shih and H.W. Pickering, *J. Electrochem. Soc.* **134** (1987) 1949.
3. A.-M. Beccaria, *J. Crousier Br. Corros. J.* **24** (1989) 49.
4. C. Kato, B.G. Ateya, J.E. Castle and H.W. Pickering, *J. Electrochem. Soc.* **127** (1980) 1890.
5. H.P. Hack and H.W. Pickering, *J. Electrochem. Soc.* **138** (1991) 690.
6. S.W. Dean, *Mater. Performance* **29** (1990) 61.
7. T.Y. Chen, A.A. Moccari and D.D. Macdonald, *Corrosion* **48** (1992) 239.
8. J.N. Alhajji and M.R. Reda, *J. Electrochem. Soc.* **141** (1994) 1432.
9. S. Martinez, *Mater. Chem. Phys.* **77** (2003) 97.
10. S. Martinez and I. Štern, *Appl. Surf. Sci.* **199** (2002) 83.
11. M.R. Reda and J.N. Alhajji, *Ind. Eng. Chem. Res.* **32** (1993) 960.
12. M.M. Singh, R.B. Rastogi, B.N. Upadhyay and M. Yadav, *Indian J. Chem. Techn* **6** (1999) 93.
13. Lj. Aljinović, S. Gudić and M. Šmit, *J. Appl. Electrochem.* **30** (2000) 973.
14. I. Milošev and M. Metikoš-Huković, *Corrosion* **48** (1992) 185.
15. M. Metikoš-Huković and I. Milošev, *J. Appl. Electrochem.* **22** (1992) 448.
16. I. Milošev and M. Metikoš-Huković, *Electrochim. Acta* **42** (1997) 1537.
17. R. Babić, M. Metikoš-Huković and M. Lončar, *Electrochim. Acta* **44** (1999) 2413.
18. F. Mansfeld and K.B. Oldham, *Corrosion Sci.* **11** (1971) 787.
19. O. Blajiev and A. Hubin, *Electrochim. Acta* **49** (2004) 2761.
20. F. Jian, Z. Wang, Z. Bai, X. You, H.K. Fun, K. Chinnakali and I.A. Razak, *Polyhedron* **18** (1999) 3401.
21. M. Lieder, *Electrochim. Acta* **49** (2004) 1813.
22. L.N. Mazalov, N.V. Bausk, S.B. Erenburg and S.V. Larionov, *J. Struct. Chem.* **42** (2001) 784.
23. B. Macias, M.V. Villa, E. Chicote, S. Martin-Velasco, A. Castineiras and J. Borras, *Polyhedron* **21** (2002) 1899.
24. C.R. Lee, L.Y. Tan and Y. Wang, *J. Phys. Chem. Solids* **62** (2001) 1613.
25. H. Tamura, N. Ito, M. Kitano and S. Takasaki, *Corros. Sci.* **43** (2001) 1675.
26. H.C. Chang and E. Matijević, *J. Colloid Interf. Sci.* **92** (1983) 479.
27. R. Espinosa, I. Zumeta, J.L. Santana, F. Martinez-Luzardo, B. Gonzalez, S. Docteur and E. Vigil, *Sol. Energ. Mat. Sol. C* **85** (2005) 359.
28. C. Alonso, M.J. Pascual, A.B. Salomon, H.D. Abruna, A. Gutierrez, M.F. Lopez, M.C. Garcia Alonso and M.L. Escudero, *J. Electroanal. Chem.* **435** (1997) 241.
29. V.P.S. Perera, G.K.R. Senadeera and K. Tennakone, *J. Colloid. Interf. Sci.* **265** (2003) 428.
30. M.G. Burnett, C. Hardacre and H.J. Mawhinney, *Phys. Chem. Chem. Phys.* **4** (2002) 3828.
31. Yu.I. Kuznetsov, 7th European Symosium on Corrosion Inhibitors (7SEIC) Ann. Univ. Ferrara, N.S., Sez. V, Suppl. N. 9 (1990) 1.
32. N. Ochoa, F. Moran, N. Pebere and B. Tribollet, *Corros. Sci.* **47** (2005) 593.
33. B. Muller, *Corros. Sci.* **46** (2004) 159.
34. M.M. Singh, R.B. Rastogi and B.N. Upadhyay, *Corrosion* **50** (1994) 620.
35. R. Babić, M. Metikoš-Huković and Z. Pilić, *Corrosion* **59** (2003) 890.
36. L.J. Aljinovic, M. Smith, V. Gotovac and Z. Hell, 7th European Symosium on Corrosion Inhibitors (7SEIC) Ann. Univ. Ferrara, N.S., Sez. V, Suppl. N. 9 (1990) 1091.
37. Y.S. Chu, I.K. Robinson and A.A. Gewirth, *J. Chem. Phys.* **110** (1999) 5952.